UNIVERSIDADE DE SÃO PAULO

INSTITUTO DE FÍSICA
CAIXA POSTAL 20516
01498 - SÃO PAULO - SP
BRASIL

PUBLICAÇÕES

IFUSP/P-620

EXPERIMENTAL TECHNIQUES USED IN THE MEASUREMENTS OF THE FUSION CROSS SECTION FOR THE $^{63,65}Cu+^{16}O$ SYSTEMS

D. Pereira, J.C. Acquadro, O. Sala, L.C. Chamon, C.A. Rocha, G. Ramirez and C. Tenreiro

Instituto de Física, Universidade de São Paulo

Dezembro/1986

EXPERIMENTAL TECHNIQUES USED IN THE MEASUREMENTS OF THE FUSION CROSS SECTION FOR THE $^{63,65}Cu+^{16}O$ SYSTEMS

D. Pereira, J.C. Acquadro, O. Sala, L.C. Chamon+,
C.A. Rocha*, G. Ramirez** and C. Tenreiro*

Instituto de Física da USP
Departamento de Física Nuclear
Caixa Postal 20516
01498 - São Paulo, SP - BRASIL

ABSTRACT

In this paper we describe the experimental techniques used in the measurement of evaporation residue cross sections for the systems $^{63,65}Cu+^{16}O$. These measurements have been carried out using the time of flight method in conjunction with an electrostatic deflector to removal the beam like particles.

RESUMO

No presente trabalho são descritas as técnicas experimentais utilizadas nas medidas da secção de choque de fusão nuclear para os sistemas $^{63,65}Cu+^{16}O$. Nestas medidas foi utilizada a técnica da medida do tempo de vôo dos produtos de reação, associada a um defletor eletrostático que tem a finalidade de separar os produtos de fusão das partículas espalhadas elasticamente.

+ Post-graduate fellowship from CNPq
* Post-graduate fellowship from FAPESP
** Post-graduate student from University of Chile

EXPERIMENTAL TECHNIQUES USED IN THE MEASUREMENTS OF THE FUSION CROSS SECTION FOR THE $^{63,65}Cu+^{16}O$ SYSTEMS

D. Pereira, J.C. Acquadro, O. Sala, L.C. Chamon+,
C.A. Rocha*, G. Ramirez** and C. Tenreiro*

Instituto de Física da USP
Departamento de Física Nuclear
Caixa Postal 20516
01498 - São Paulo, SP - BRASIL

I. INTRODUCTION

In the São Paulo Pelletron Laboratory, we have initiated a program to measure fusion cross section for the systems $^{63,65}Cu+^{16}O$. In order to detect and to obtain the mass identification of the evaporation residues following the fusion process the time of flight method was adopted in conjunction with an electrostatic deflector[1,2,3] capable of separating the evaporation residues from the beam like particles. In order to reduce the number of scattered beam particles entering the detection system, the beam defining slits and collimators were removed and replaced by an on-target beam positioner developed in our Laboratory.

The present paper gives a brief description of the techniques employed in the measurements of the above mentioned fusion cross sections.

+ Post-graduate fellowship from CNPq
* Post-graduate fellowship from FAPESP
** Post-graduate student from University of Chile

II. THE MODIFIED SCATTERING CHAMBER FOR T.O.F.

The scattering chamber[4] installed at our laboratory in 1977 for T.O.F. measurements, was modified for the present experiments and a schematic view of the apparatus is shown in figure I. In this figure is indicated the T=0 detector, a thin scintillator foil (~70μg/cm² thick) of the plastic NE-111 with a spherical mirror coupled to a fast photomultiplier (RCA-8575). It is worth mentioning that the scintillator foil has an important effect in the equilibrium of the average atomic charges state of the reaction products. Also shown is the electrostatic deflector, a set of two retangular plates, 3 cm wide and 20 cm long, with a gap of 1cm between them. For the energy range of our accelerator (up to 72 MeV for the ^{16}O beam) and the geometry of our apparatus, a few kilovolts applied to the electrostatic plates are enough to separate the beam particles from the evaporation residues in the E detector. The E detector, a 50 mm² area silicon surface barrier detector, can be cooled and moved perpendicular to the electrostatic deflector axis without vacuum breakage. Finally, the beam on target positioner, which utilizes the secondary electrons emitted from the target upon passage of the beam, is shown. The secondary electron currents (I_1,I_2) are collected in two copper plates positioned at the distance of 1.6 mm upstream from the target. The beam position on the target is determined[5] by the normalized ratio

$(I_1-I_2)/(I_1+I_2)$. By measuring this ratio, it is also possible to control automatically the on-target beam position, using the steering magnet placed in front of the scattering chamber, in a feedback procedure.

It is important to mention that one limitation of our system is the position of the T=0 detector. Without involved mechanical changes we found it is difficult to locate it downstrean from the electrostatic deflector. Despite this inconvenience it was found that the T=0 detector is able to support a counting rate up to 1 MHz, which is adequate for the proposed experimental conditions.

III. EXPERIMENTAL RESULTS

III.a. The Effect of the Electrostatic Deflector on the Collection Efficiency

A series of measurements intended to check the effect of the electrostatic deflection plates on the overall detection efficiency should be mention here. The curves in figure II show, for the system $^{nat}Cu+^{16}O$ at $\theta_{LAB} = 7^{o}$ and E_{LAB} (^{16}O) = 48 and 64 MeV, the normalized* yeld of the evaporation residues as function of the voltage applied to the electrostatic deflector. In these measurements the center of

* The data was normalized with respect to a monitor counter positioned at the fixed angle of $\theta_{LAB} = 26,7^{o}$.

the E detector was displaced 13 mm from the symmetric axis of the electrostatic deflector. The results shown in figure II indicated the optimum voltage applied in the electrostatic deflector for the full collection of the evaporation residues in the solid angle defined by the apparatus. This yield was found to be the same as for the situation in which the E detector was positioned on the symmetric axis of the electrostatic deflector, without voltage being applied. The measured optimum voltage coincides with the calculated value using the equilibrated average atomic charge state[6] of the evaporation residues and the geometry of our apparatus.

III.b. **Fusion Data for the Systems $^{63,65}Cu+^{16}O$**

In this section some experimental results of the fusion process for the systems $^{63,65}Cu+^{16}O$ are presented. In figure III is shown a typical E vs T.O.F. spectrum for the $^{63}Cu+^{16}O$ system ($E_{LAB}(^{16}O)$ = 64 MeV and $\theta_{LAB} = 7^{o}$). In this spectrum the evaporation residues island is well defined and separated from other groups of mass. The average velocity of this group coincides with the velocity of the compound nucleus formed in the $^{63}Cu+^{16}O$ reaction at E_{LAB} = 64 MeV. In this spectrum we can notice also the small contribution of the scattered beam (^{16}O particles) due to the removal of the slits and collimators as discussed in section II. In figure IV we presented an angular distribution for the evaporation residues

from the $^{65}Cu+^{16}O$ system (E_{LAB} = 60 MeV). This angular distribution has been measured for both positive and negative scattering angles and illustrated the good angular symmetry of our experimental apparatus.

III.c. **The On-Target Beam Position Stability**

As discussed in section II, the beam position on the target is determined measuring the secundary electrons currents (I_1 and I_2). Figure V shows the variation of the normalized ratio $(I_1-I_2)/(I_1+I_2)$ as function of the position of the beam on the target. On the basis of these data, we have found that the beam position stability was very good and even disconnecting the feed back control circuit the overall stability of the accelerator system was good enough to maintain the beam position almost unaffected during the runs.

The Table I indicates the main characteristics of the time of flight detecting system.

IV. **CONCLUSIONS**

In conclusion it was shown that with simple modifications in our old scattering chamber and the introduction of some new techniques, it was possible to measure evaporation residues cross sections in medium heavy systems like $Cu+^{16}O$ in the energy range of our accelerator.

TABLE I. Main characteristics of the T.O.F. system:

- geometrical solid angle - 5×10^{-2} m.s.r.
- acceptance angle - $\pm0.24^{o}$
- time resolution* - 1 ns
- energy resolution* - 2-3%
- flight path - 74 cm
- scattering angle measureable range - $2^{o}\leq\theta_{LAB}\leq150^{o}$
- typical operating voltages on the electrostatic
- deflector - 2-3 kV

* E detector at room temperature.

REFERENCES

1. S. Beghini, C. Signorini, S. Lunardi, M. Morando F. Fortuna, M. Stefanini, W. Meczynski and R. Pengo
   Nuclear Instruments and Methods A239, 585 (1985).

2. M. Dahling, W. Bonin, E. Kankeleit and H. Backe
   Nuclear Instruments and Methods A215, 513 (1984).

3. W.S. Freeman, H. Ernst, D.F. Geesaman, W. Henning, T.J. Humanik, W. Kühn, J.P. Schiffer, B. Zeidman and F.W. Prosser
   Physics Review C8, 919 (1983).

4. N.D.Vieira Jr.
   Master Thesis - University of São Paulo, 1979.

5. J.C. Acquadro, U. Schnitter, A.P. Teles, D. Pereira, O. Sala and P.A.B. Freitas
   Nuclear Instruments and Methods A244, 229 (1986).

6. H.D. Betz
   Review of Modern Physics, 44, 465 (1972).

Figure Captions

Figure I. A schematic view of the experimental apparatus.

Figure II. Behaviour of the normalized yield of the evaporation residues for the $^{63}Cu+^{16}O$ system, at E_{LAB} = 48MeV and 64 MeV ($\theta_{LAB} = 7^{o}$), as function of the applied voltage on the electrostatic deflector. In the figure are indicate the optimum voltages (vopt) corresponding to the respective maximum normalized yield (see text).

Figure III. Typical E vs T.O.F. spectrum for the $^{63}Cu+^{16}O$ system at E_{LAB} = 64 MeV and $\theta_{LAB} = 7^{o}$. In the figure is indicated the velocity of the center of mass of the compound system formed in the reaction. The voltage on the electrostatic deflector was fixed at 2.75 kV.

Figure IV. Angular distribution for the evaporation residues for the $^{65}Cu+^{16}O$ system (E_{LAB} = 60 MeV). The curve drawn in the figure is the "best-fit" using an exponential expression for $(d\sigma/d\Omega)_{LAB}$

Figure V. Behaviour of the normalized I_1-I_2/I_1+I_2 current difference as a function of the beam position on the target.

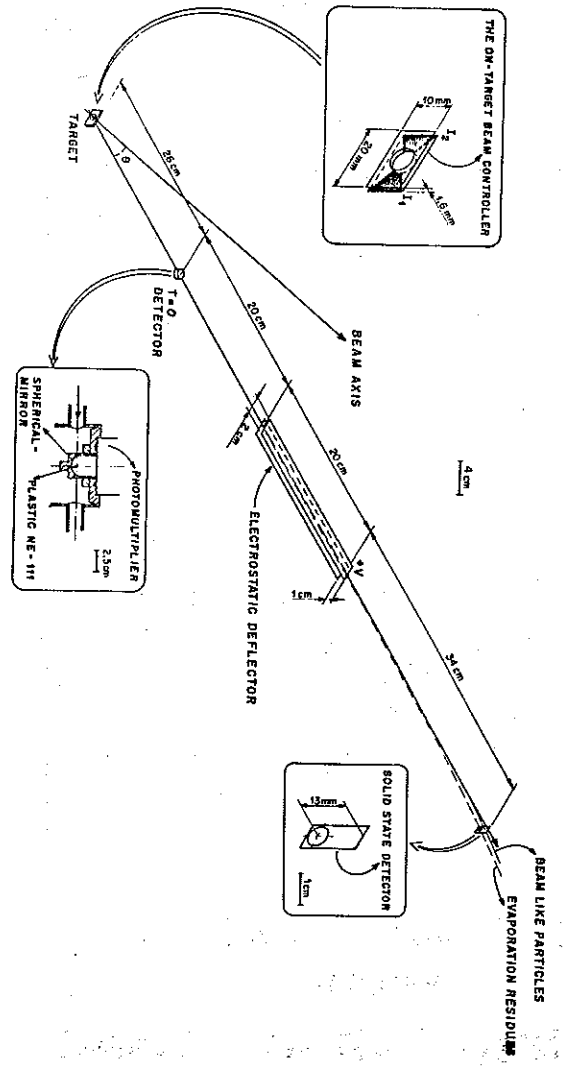

Figure 1

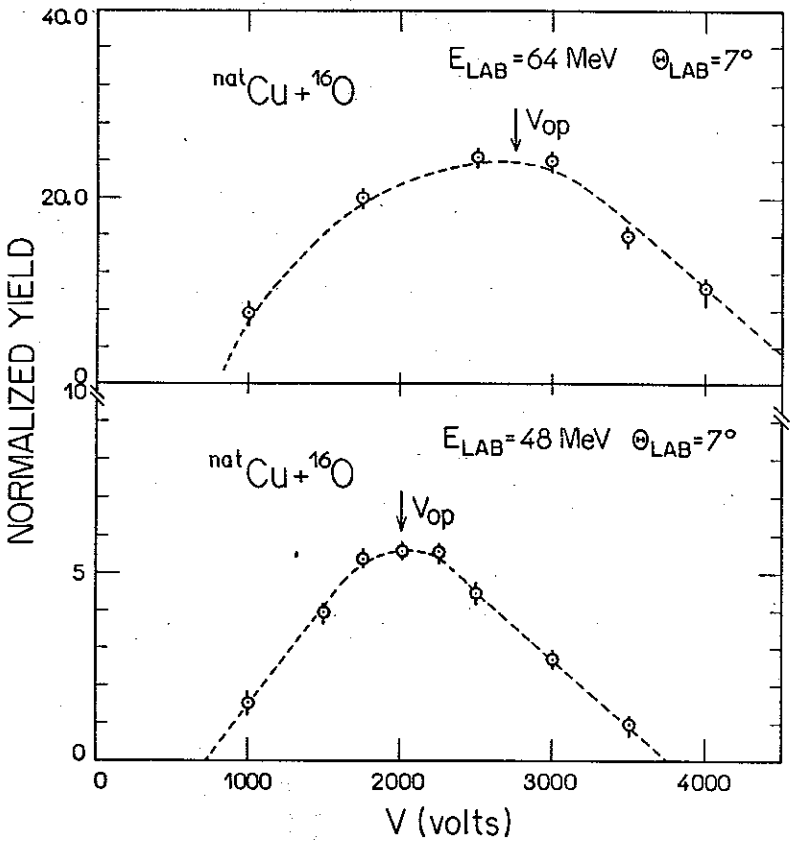

Figure 2

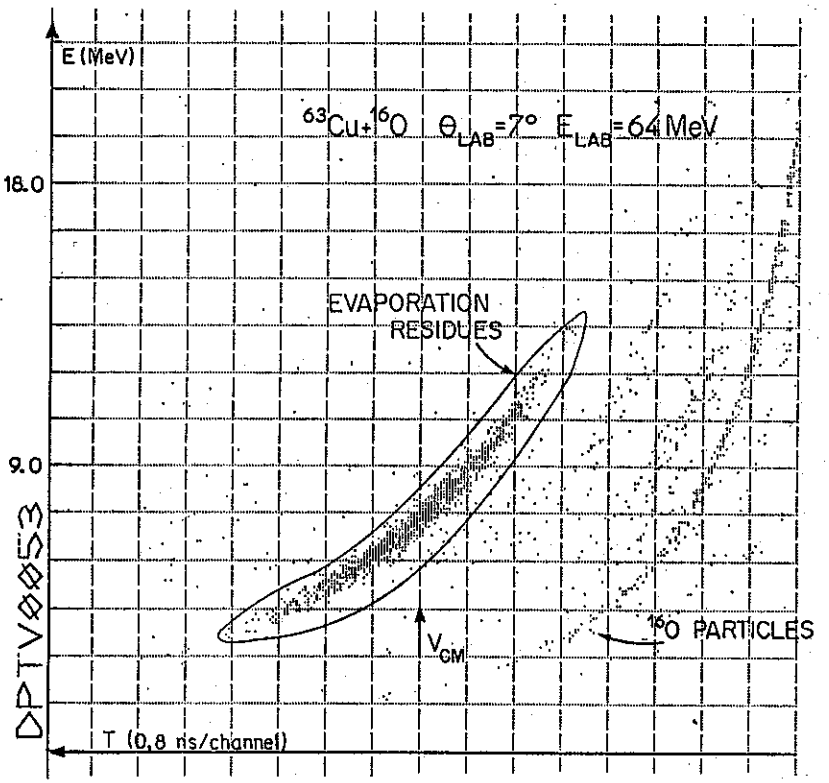

Figure 3

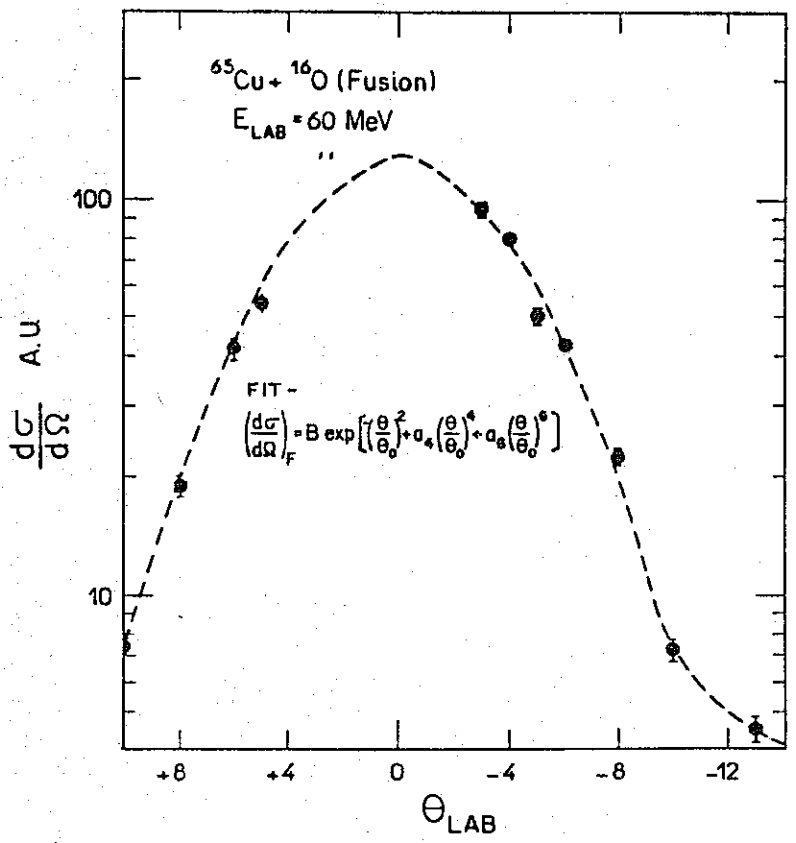

Figure 4

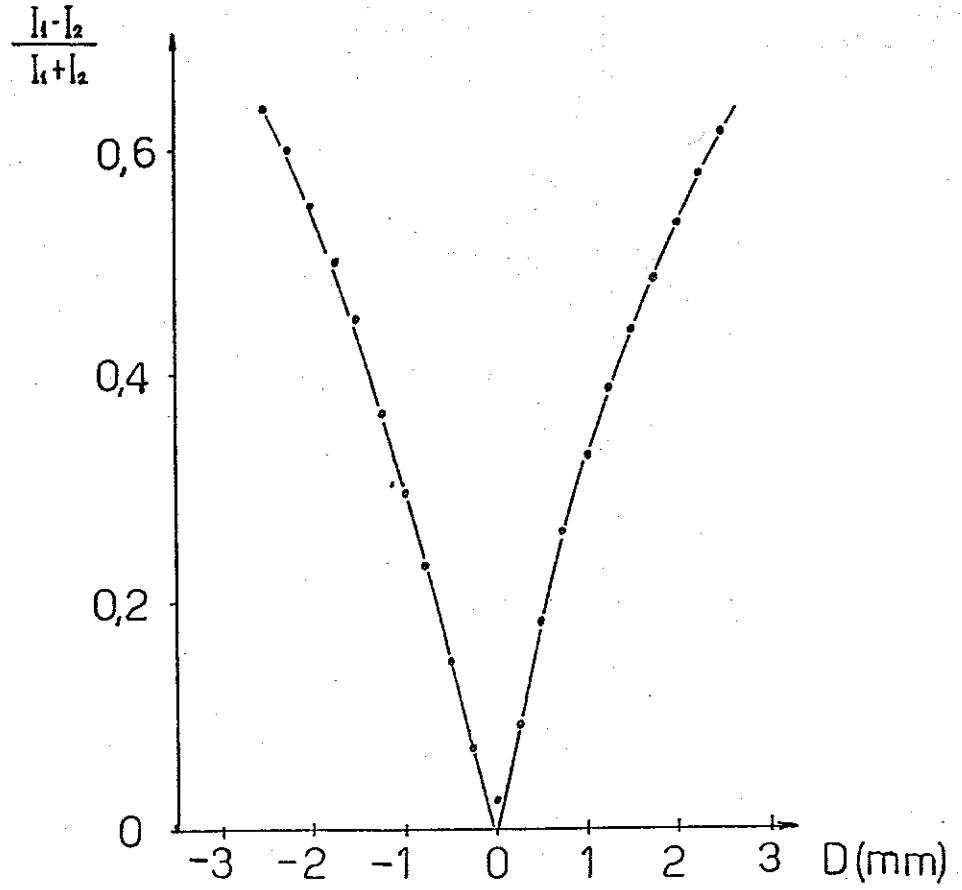

Figure 5